Korean J. Chem. Eng., 32(11), 2204-2211 (2015)
DOI: 10.1007/s11814-015-0027-9

pISSN: 0256-1115
eISSN: 1975-7220

Performance evaluation and mass transfer study of CO_2 absorption in flat sheet membrane contactor using novel porous polysulfone membrane

Nima Nabian*, Ali Asghar Ghoreyshi*,†, Ahmad Rahimpour*, and Mohsen Shakeri**

*Chemical Engineering Department, Babol University of Technology, Babol, Iran
**Mechanical Engineering Department, Babol University of Technology, Babol, Iran
(*Received 5 August 2014 • accepted 29 January 2015*)

Abstract–The performance of gas-liquid membrane contactor for CO_2 capture was investigated using a novel polysulfone (PSF) flat membrane prepared via non-solvent phase inversion method. Polyvinyl pyrrolidone (PVP) was used as an additive in the dope solution of PSF membranes. Morphological studies by scanning electron microscopy (SEM) analysis revealed that PSF membrane with PVP has a finger-like structure, but the PSF membrane without PVP has a sponge-like structure. Also, characterization results through atomic force microscopy (AFM) and contact angle measurement demonstrated that the porosity, surface roughness and hydrophobicity of the PSF membrane increased with addition of PVP to the dope solution. Mass transfer resistance analysis, based on CO_2 absorption flux, displayed that addition of PVP to the dope solution of PSF membrane decreased membrane mass transfer resistance, and significantly improved CO_2 absorption flux up to 2.7 and 1.8 times of absorption fluxes of PSF membrane without PVP and commercial PVDF, respectively.

Keywords: CO_2 Absorption, Polysulfone, PVP Additive, Membrane Contactor, Mass Transfer

INTRODUCTION

The largest source of greenhouse gas emissions from human activities is usually from burning fossil fuels such as coal, fuel oil and natural gas for electricity production in thermal power plants as well as heat generation in industrial, commercial and residential sectors. Petroleum processing and use of petroleum based fossil fuels such as gasoline and diesel for transportation systems are the other fundamental sources of greenhouse gas generation [1-3].

Some consequences of global warming could be environmental hazards such as more droughts and floods, less ice and snow, more extreme weather incidents and rising sea levels. Water vapor, carbon dioxide, methane, nitrous oxide, ozone and CFCs are known as greenhouse gases. Among them, CO_2 is regarded as the most serious due to its high concentration in greenhouse gases and its remarkable function in enhanced greenhouse effect [4,5]. Therefore, it is essential to develop efficient separation processes to remove CO_2 from industrial off gas mixtures.

There are different kinds of CO_2 removal methods, including physical or chemical absorption, molecular sieve based adsorption, cryogenic distillation systems and membrane applications [6-8]. The conventional processes extensively used in this field are CO_2 capturing by absorption into aqueous solutions using gas/liquid contacting operations such as packed towers, bubble columns, venturi scrubbers and tray columns [9-11]. However, the most commercial one is the packed column using alkanolamines as absorbent solutions. These contacting devices suffer some drawbacks, such as large size, low specific gas-liquid interfacial area, high capital and operating cost, and also some operational problems such as flooding, channeling, entrainment, and foaming [12].

Application of membrane-based gas separation is another technique for the recovery of CO_2. Despite the development achieved by decreasing the thickness and increasing the selectivity of membranes used for this purpose, their low permeability and low mass transfer rate have limited their commercial utilization [13-15]. Thus, a novel technology known as membrane contactor has been improved, which takes advantage of both membranes and gas-liquid absorption processes and overcomes their aforementioned problems. In this way, the role of the membrane has been just a stationary interface between gas and liquid phases and does not have any function in offering the selectivity between the species of gas streams [16]. Hence, the membrane contactor furnishes a modular system with high interfacial area per unit volume, easy scale-up with independent control of gas and liquid streams and high selectivity with high mass transfer flux provided by liquid absorbent [17,18]. On the other hand, in addition to the gas phase and liquid phase mass transfer resistances, the membrane contactor module has the drawback of extra membrane mass transfer resistance, which reduces its performance. However, use of hydrophobic membranes with optimized pore size, which ensures completely gas-filled pores, can assist to minimize the membrane resistance due to the higher diffusivity of gas phase compared to liquid phase [19-21].

CO_2 removal using this technology has been extensively investigated by different membrane configurations, but most of them were devoted to hollow fiber membrane contactors [22-24] with few exceptions of flat sheet ones [25-27]. Khaisri et al. [28] compared the

†To whom correspondence should be addressed.
E-mail: aa_ghoreyshi@nit.ac.ir

performance of a gas absorption membrane system in both physical and chemical absorption studies using three common hydrophobic membranes including polytetrafluoroethylene (PTFE), polypropylene (PP) and polyvinylidene fluoride (PVDF). They found that the CO_2 absorption performance can be ranked as PTFE>PVDF> PP. Although PTFE is regarded as the most hydrophobic membrane and displays good absorption performance, it is considerably expensive, which restricts its application. Mansourizadeh et al. [29] evaluated CO_2 stripping from water through PVDF hollow fiber membrane contactor. Their results showed that the liquid phase temperature, the gas-liquid contact area and contact time are the key parameters for enhancement of CO_2 stripping efficiency. Yan et al. [30] used PP hollow fiber membrane contactor to absorb CO_2 from flue gas using potassium glycinate (PG) solution and aqueous solutions of monoethanolamine (MEA) as the absorbents. According to their obtained data, the aqueous PG solution has a lower potential of membrane wetting after continuously steady operation for 40 h. Lv et al. [31] assessed the efficiency of super hydrophobic PP hollow fiber membrane contactors for CO_2 absorption with MEA solution. In addition to the membrane material, its structure is an important factor in the success of membrane contactor technology. Therefore, some researches have been carried out on hollow fiber membrane modifications using different additives in the dope solution of other membrane materials [32,33]. Ghasem et al. used o-xylene as an additive of dope solution in the preparation of polyethersulfone hollow fiber membranes and found that this additive reduced water permeability and membrane pore size [34]. Polysulfone (PSF) membrane has been applied in different membrane separation processes and is a good candidate for membrane gas absorption due to its relatively strong hydrophobicity, good chemical resistance and high heat resistance. Rahbari et al. studied the effect of glycerol as an additive to the spinning dope of PSF hollow fiber membranes which resulted in a membrane with high permeability and low mass transfer resistance [35]. To the best of our knowledge, no research has been done on the absorption of CO_2 using PSF flat sheet membrane contactors. Also, addition of polyvinyl pyrrolidone (PVP) to the dope solution of PSF flat membrane contactors for CO_2 absorption has not been reported yet in the literature. Therefore, the present work focuses on the CO_2 absorption rates in a novel PSF flat sheet membrane using distilled water as absorbent. The absorption performance of different fabricated PSF and commercial PVDF flat membranes was compared. Also, the effects of liquid flow rates on CO_2 absorption fluxes and mass transfer resistances during the experiments were determined.

THEORY

1. Governing Equations for Mass Transfer

According to the film model, overall mass transfer in membrane contactor module has been considered as resistance in the series model, which takes place in three steps, including mass transfer from the bulk gas phase into membrane surface, mass transfer through the membrane pores and mass transfer from the membrane-liquid interface into bulk liquid phase. Fig. 1 shows schematically the concentration profile across the hydrophobic microporous membrane, and the following equation can be used to express CO_2 flux

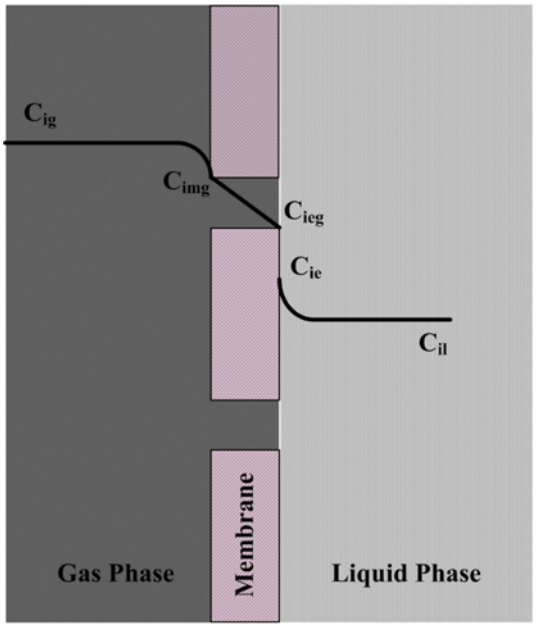

Fig. 1. Concentration profile across the hydrophobic microporous membrane.

(mol/m^2·s) through a flat sheet membrane contactor [36]:

$$J_i=K_l(C_i^{id}-C_{il})=k_{ig}(C_{ig}-C_{img})=k_{im}(C_{img}-C_{ieg})=K_{il}(C_{ie}-C_{il}) \quad (1)$$

where K_l is an overall mass transfer coefficient of the liquid phase (m/s); k_{ig}, k_{im} and k_{il} are the mass transfer coefficients (m/s) in the gas, membrane and liquid phases for the species CO_2, respectively; C_{ig} and C_{il} are CO_2 concentrations (mol/m^3) in the gas and liquid phase, respectively; C_{img}, C_{ieg} and C_{ie} are CO_2 concentrations at the gas-membrane interface, the gas-liquid interface and the liquid-gas interface, respectively; and C_i^{id} is CO_2 concentration in the liquid phase ideally in equilibrium with its concentration in the gas phase.

Based on the resistance in series model, the overall liquid phase mass transfer coefficient (K_l) can be explained by the following equation [36]:

$$1/K_l=1/k_{il}+1/(k_{im}H_e)+1/(k_{ig}H_e) \quad (2)$$

where H_e is dimensionless Henry 's law constant for CO_2.

Individual mass transfer coefficients of the liquid phase and the gas phase can be predicted by equations which have been presented in the literature [37,38]. Furthermore, the membrane mass transfer coefficient in an operation without wetting can be calculated using Eq. (3) [39]:

$$k_{im}=\frac{\varepsilon_m D_{ie}}{\tau_m t_m} \quad (3)$$

where ε_m is the membrane porosity, D_{ie} is the effective diffusivity, τ_m and t_m are membrane tortuosity and membrane thickness, respectively.

2. Wilson Plot Method

The Wilson plot is an alternative technique for evaluating the membrane resistance [40]. The mass transfer resistance of the liquid phase is dependent on the liquid velocity (u), and the gas phase

mass transfer resistance can be neglected if pure CO_2 is used as the feed gas in physical gas absorption membrane systems [37]. A graph of $1/K_l$ versus $1/u^{\alpha}$, called a Wilson plot, yields a straight line with an intercept of the membrane resistance. The empirical α value of the graph is a constant resulting in the best straight line.

EXPERIMENTAL

1. Materials

The casting solution was prepared using PSF beads (PS Mn: 22,000 Da, Sigma-Aldrich) as the membrane substrates polymer, N,N-dimethylformamide (DMF 99.5%, Dae Jung, Korea) as the solvent and Polyvinyl pyrrolidone (PVP, with Mw=25,000 g/mol, Merck) as additive and pore former. Sodium dodecyl sulfate (SDS, Merck) was used in the precipitation bath of fabricated membranes. Also, the commercial polyvinylidine fluoride sheet membrane (PVDF-MFB) was purchased from Sepro Membranes (USA).

2. Synthesis of PSF Flat Sheet Membranes

PSF membranes were fabricated using two different dope solutions. 18 wt% PSF beads with and without 1 wt% PVP (PSF-PVP and PSF samples) were stirred in the DMF at 298.15 K for at least 8 h until the solution became homogeneous. The dope solution was then degassed for 12 h at room temperature. The polyester non-woven fabric with thickness of about 100 μm was attached to a clean glass plate, and the dope solution was then spread onto the polyester fabric using a casting knife. The whole composite was immediately immersed in the precipitation bath containing distilled water, 0.1 wt/vol% SDS and 2 wt/vol% DMF for 30 min. Then, the membranes were washed and stored in a water bath for at least one day to leach out the residual solvents and additives completely. As the final stage, the membrane was dried by placing between two sheets of filter paper for 24 h at room temperature.

3. Membrane Characterizations

To characterize the morphological properties of prepared membranes, scanning electron microscopy (SEM model: KYKY-EM3200) operating at 24 KV was used for surface and cross section scanning. The samples were coated with a gold layer before the examination. The membranes were fractured in liquid nitrogen for the cross section scanning. Atomic force microscopy (AFM model: Easyscan2 Flex) was used to determine the surface morphologies and the roughness of the PSF membranes. The surfaces of the membranes were imaged in scan size of 5 μm×5 μm at atmospheric pressure. For each membrane, the reported roughness value is the average of roughness values of three scanned images. The mean roughness value (S_a) measured by an AFM is defined as [41]:

$$S_a = \frac{1}{LW}\int_0^L\int_0^W |f(x, y)|dxdy \tag{4}$$

where f(x, y) is the surface relative to the center plane, L and W are the surface dimensions. Based on the pore size distribution function (F_r) obtained by AFM data, the mean pore size of the membranes (r_{ave}) can be estimated through Eq. (5) [41]:

$$r_{ave} = \frac{\int_{r_{min}}^{r_{max}} rF_r dr}{\int_{r_{min}}^{r_{max}} F_r dr} \tag{5}$$

By measuring the dry mass (m_{dry}) and wet mass (m_{wet}) of membranes, membrane porosity (ε) can be calculated using Eq. (6) [42]:

$$\varepsilon = \frac{\frac{m_{wet}-m_{dry}}{\rho_w}}{\frac{m_{wet}-m_{dry}}{\rho_w}+\frac{m_{dry}}{\rho_P}} \times 100 \tag{6}$$

where ρ_P is the density of the polymer (1.25 g/cm^3 for PSF) and ρ_w is the density of water.

A simple method to determine the membrane's ability to prevent the liquid phase penetration into membrane pores is contact angle measurement [43]. The sessile drop method was applied by a contact angle goniometer (Dataphysics OCA 15, Germany) to measure the contact angle of distilled water on fabricated flat sheet membranes. The volume of a single water drop created on the membrane surface was 4 μl for each test. Contact angles were obtained by repeating the measurement for three times and average values were reported. Specifications of two fabricated PSF membranes are listed in Table 1.

Table 1. Characteristics of fabricated PSF flat membranes

Membrane	Mean pore size r_{ave} (nm)	Porosity ε (%)	Roughness S_a (nm)	Water contact angle
PSF	129.29	64.22	7.38	69.6
PSF-PVP	117.91	67.63	13.92	77.2

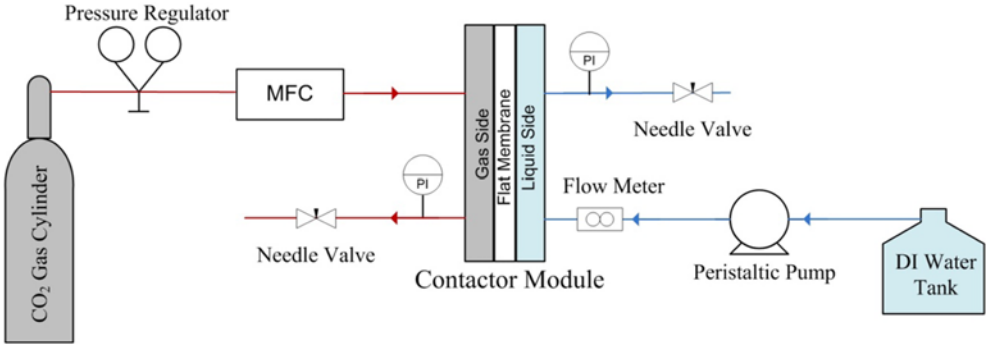

Fig. 2. Experimental setup of CO_2 absorption using membrane contactor module.

4. CO_2 Absorption Experiment

A schematic representation of experimental setup of flat sheet membrane contactor for measuring CO_2 flux is shown in Fig. 2. The membrane contactor module consisted of two flow field plates and a membrane interposed between them. In this study, the serpentine channels were formed on the flow field plates for directing gas and liquid streams. The width and the depth of the channels are 1.0 mm. Pure CO_2 as the feed gas was used on one side of the membrane, and distilled water as the liquid absorbent was used on the other side of the membrane in the constructed module. To obtain the best performance, all the experiments were conducted in a countercurrent mode operation. The equipment used in the gas line of the setup consists of a CO_2 gas cylinder, a pressure regulator, a mass flow controller (MFC), a pressure gauge and a needle valve. In all experiments, CO_2 was introduced into the contactor module before the liquid stream injection to prevent membrane wetting phenomena. Gas flow rates were controlled by a mass flow controller (Dwyer GFC-1107, USA) at 298.15 K and atmospheric pressure. The absorbent solution (water) flowed in the liquid line by a peristaltic pump (Thomas SR25, Germany), and the liquid flow was varied between 3 and 12 ml/min. To avoid dispersion of gas bubbles into the liquid, a pressure gauge and a needle valve were placed in the liquid line to regulate the differential pressure between the gas and the liquid phase in the range of 2-4 psig. At the steady state condition, which was obtained after at least 20 min of each run, the mass transfer flux was obtained by the following equation:

$$J_i = \frac{Q_L(C_{il,\,out} - C_{il,\,in})}{A_m} \tag{7}$$

where Q_L is liquid volumetric flow rate (m^3/s); A_m is membrane mass transfer surface area (m^2); $C_{il,\,out}$ and $C_{il,\,in}$ are CO_2 concentrations in the outlet and inlet liquid respectively (mol/m^3). As pure distilled water was used as the absorption liquid, CO_2 concentration was zero at the module inlet. CO_2 content at the module outlet was measured by the chemical titrimetric method in which sodium hydroxide solution was used as a titrant with phenolphthalein as an indicator [33]. For each experiment, the reported mass transfer flux was the average flux value of three samples, taken under the same operating conditions. Based on the mass balance for the liquid phase, the overall mass transfer coefficient of liquid phase was calculated through Eq. (8) [44]:

$$K_L = -\frac{Q_L}{A_m}\ln\left(\frac{HC_{ig} - C_{il,\,out}}{LHC_{ig} - C_{il,\,in}}\right) \tag{8}$$

Two fabricated PSF membranes and the commercial PVDF membrane were separately placed in the contactor module and their results were compared.

RESULTS AND DISCUSSIONS

1. Characterization Results of PSF Membranes

Fig. 3 shows morphology pictures of the cross-section and sur-

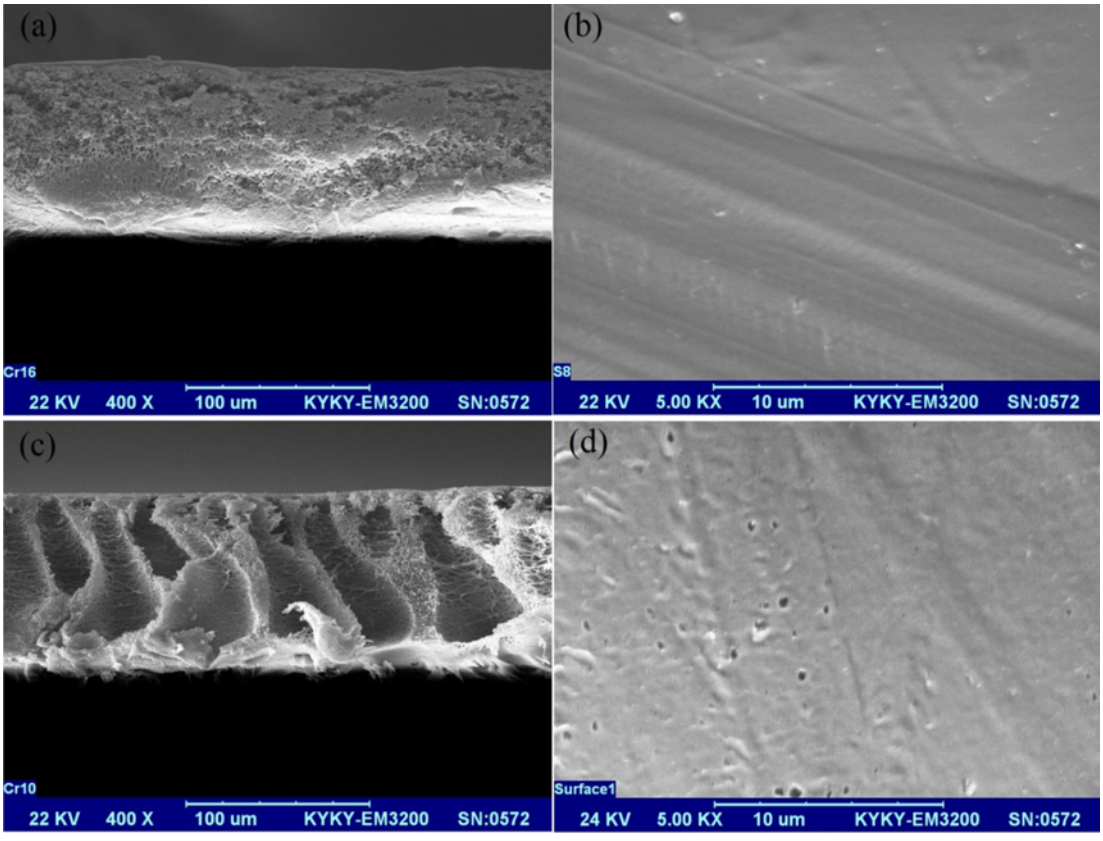

Fig. 3. SEM images of fabricated PSF flat membranes (a) cross section of PSF (b) surface of PSF (c) cross section of PSF-PVP and (d) surface of PSF-PVP.

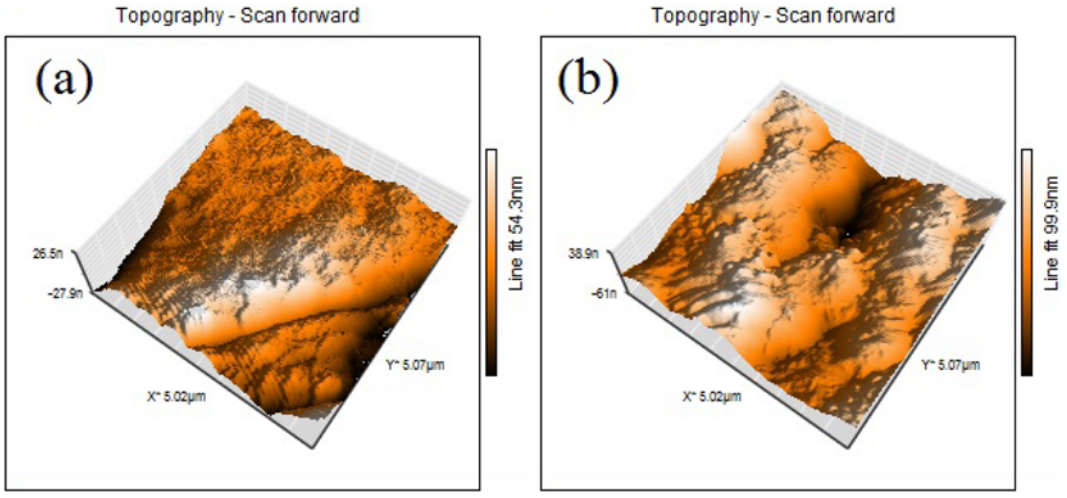

Fig. 4. AFM images of fabricated PSF flat membranes (a) PSF (b) PSF-PVP.

face of PSF flat sheet membranes fabricated with and without PVP as an additive to the dope solution. As can be seen in Figs. 3(a) and 3(c), the PSF-PVP membrane has a finger-like structure while the PSF membrane without PVP has a sponge-like structure. This phenomenon can be attributed to the increased viscosity of dope solution due to addition of PVP, which reduced the mutual diffusion between solvent and non-solvent [45]. Also, a decrease in miscibility of dope solution, which resulted in faster precipitation of dope solution in non-solvent phase via inversion method, changed the morphology of PSF membrane from a sponge-like for slow phase inversion to finger-like structure [46]. According to Figs. 3(b) and 3(d), the porosity and surface roughness of the membrane increased with addition of PVP to the dope solution, which is also confirmed by the data represented in Table 1.

Fig. 4 displays the three-dimensional AFM images of PSF and PSF-PVP membranes. The dark and bright sections in AFM pictures are representative of depression (membrane pores) and nodules, respectively. Besides, the roughness of the substrate is assigned to the height of the surface's lumps [47]. It is obvious that addition of PVP changed the membrane surface morphology and increased the surface roughness as presented in Table 1. Also, the porosity of the PSF membrane was increased from %64.2 to %67.6 by addition of PVP. Porosities higher than this value [48] and lower than this value [49] were reported in the literature for hollow fiber PSF membranes. In general, the porosity of a fabricated membrane is completely dependent on the synthesis condition such as polymer concentration, additives, doping material and type of the solvent.

In addition to the morphological studies of PSF membranes, the effect of PVP on the membrane hydrophobicity can be evaluated by comparing the data of water contact angles represented in Table 1. With addition of PVP to the dope solution, the contact angle of PSF sample increased, and hence the more hydrophobic flat PSF membrane was fabricated. As the hydrophobicity of the membrane increased, the probability of membrane wetting decreased, which is a good parameter for CO_2 removal efficiency.

2. Analysis of CO_2 Absorption Performance

The absorption flux of CO_2 using fabricated PSF membrane without PVP was determined at constant various absorbent flow rates to evaluate the dependency of the membrane contactor performance on the liquid phase mass transfer resistance. A constant gas flow rate of 1,000 ml/min was selected for this test. As shown in Fig. 5, the absorption flux of CO_2 increased by increasing the liquid velocity due to the decrease of liquid boundary layer and the increase of liquid mass transfer coefficient. Similar trends were also reported for CO_2 absorption flux using water as absorbent in commercial PP and PTFE membrane contactor [35,50]. An increase in the liquid flow rate led to the enhancement of the CO_2 mass transfer rate.

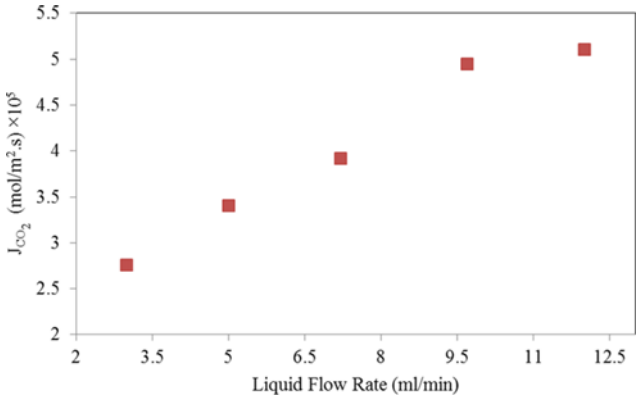

Fig. 5. CO_2 absorption fluxes at various liquid flow rates using PSF membrane without PVP (constant gas flow rate of 1,000 ml/min).

3. Comparing the Performance of Different Membranes

To investigate the capability of different membranes in CO_2 absorption, experiments were also conducted in flat sheet membrane contactor module using commercial PVDF membrane and PSF-PVP membrane (see Fig. 6). As discussed earlier in section 4.2, it is clear that CO_2 absorption fluxes of all membranes were increased by increasing the liquid flow rate from 3 to 12 ml/min. The absorption flux of PSF flat membrane was considerably enhanced with addition of PVP and was greater than both the purchased commercial PVDF and PSF membrane without PVP. At the absorbent

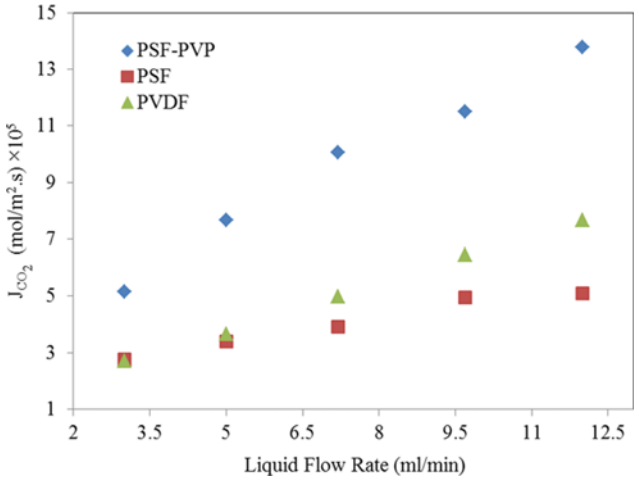

Fig. 6. CO_2 absorption fluxes at various liquid flow rates using PSF membrane without PVP, PSF-PVP and commercial PVDF membranes.

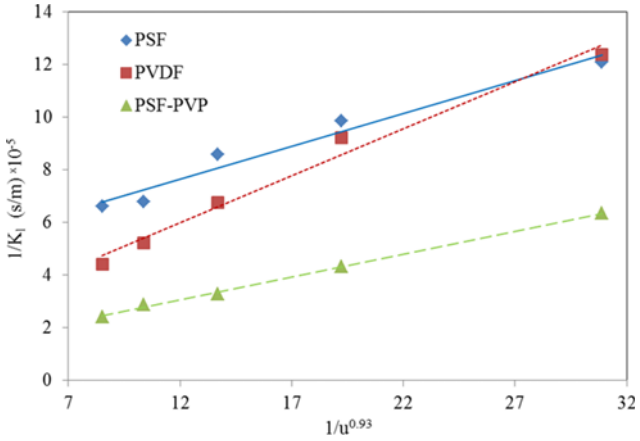

Fig. 7. Wilson plot for pure CO_2 absorption using distilled water.

flow rate of 12 ml/min, CO_2 absorption flux of PSF-PVP membrane was 2.7 and 1.8 times higher than absorption fluxes of the PSF membrane without PVP and commercial PVDF, respectively. This phenomenon can be ascribed to the modified structure of PSF-PVP membrane. The increase in the porosity of the PSF membrane with addition of PVP resulted in higher gas-liquid contact area and higher permeability, which both of them are favorite factors in a membrane contactor. As discussed before, the mean pore size of membrane decreased and its contact angle increased with addition of PVP. Therefore, the wettability resistance of membrane increased, which also improved the membrane performance for CO_2 absorption.

Furthermore, with an increase in liquid flow rate, CO_2 absorption flux of PSF-PVP membrane increased more rapidly in comparison to the PSF membrane without PVP. As the absorbent flow rate changed from 3 to 12 ml/min, an enhancement of 166% was observed in CO_2 flux of PSF-PVP membrane, while CO_2 flux of the PSF membrane without PVP increased just 85%, which can be attributed to gradual membrane wetting due to the higher mean pore size and the lower membrane hydrophobicity.

CO_2 absorption flux of commercial PVDF membrane was lower than that of the PVP-modified PSF membrane synthetized in this study. It can be related to the probable symmetric structure of PVDF membrane with low porosity, resulting from temperature induced phase separation (TIPS) method which is usually applied for the fabrication of commercial membranes.

4. Analysis of Membrane Resistance

According to resistance in series model presented in Eq. (2), by neglecting gas phase mass transfer resistance in flat sheet membrane contactor, because of the use of CO_2 as the pure feed gas, the membrane mass transfer can be determined by using the Wilson plot shown in Fig. 7. The best straight line to the data of $1/K_l$ versus $1/u^{\alpha}$ was obtained from α equals to 0.93. Yang et al. [51] reported a similar relationship of $1/K_l$ with $1/u^{0.93}$ to evaluate the liquid stream in designing hollow fiber contactors. The membrane mass transfer resistance calculated from the intercept of the plot shows the contribution of membrane resistance in overall mass transfer resistance. Membrane resistances, equations and regression coefficients of different membranes are reported in Table 2.

According to these data, the membrane mass transfer resistance of the PSF membrane without PVP decreased to approximately 20% of its value with addition of PVP in the dope solution of PSF-PVP membrane. This confirms better performance of PSF-PVP membrabe in contactor module. At the liquid velocity of 0.025 m/s, nearly 15% of the total resistance can be attributed to the mass transfer resistance of PSF-PVP membrane. So, the mass transfer resistance of the liquid phase can be regarded as 85% of the total resistance neglecting the gas phase resistance. Meanwhile, the contribution of commercial PVDF and PSF without PVP membrane resistances in overall resistance was 13% (nearly the same as PSF-PVP membrane) and 47%, respectively. As it can be seen in Fig. 7, the overall mass transfer resistance decreased with an increase in the liquid velocity; consequently, the contribution of the membrane resistance increased. The results revealed that the contribution of the membrane resistance for PSF-PVP membrane increased 2.66 times by increasing the liquid velocity from 0.025 to 0.1 m/s. This can be attributed to the disturbance of the boundary layer in the liquid phase with an increase in the velocity. Using the Wilson plot for evaluation of mass transfer resistance has been reported in the lit-

Table 2. Equation and membrane resistance obtained by Wilson plot

Membrane	Equation	R-squared value	Membrane resistance (s/m)
PSF	y=24929 x+465948	0.9655	465948
Commercial PVDF	y=35716 x+169268	0.9829	169268
PSF-PVP	y=17401 x+97482	0.9982	97482

erature [52]. Lin et al. used the Wilson plot for determination of mass transfer resistance during CO_2 absorption by alkanolamine absorbents in PVDF and PP membrane contactors [53].

CONCLUSION

The performance of flat sheet membrane contactors for CO_2 absorption was investigated by using a novel porous PSF membrane fabricated via phase inversion method. PVP was added to the dope solution of PSF membrane, and CO_2 mass transfer through both membranes was compared to the commercial PVDF membrane. The addition of PVP to the dope solution changed the morphology of membrane from a sponge-like to finger-like. The effect of liquid flow rates on the mass transfer flux was evaluated, and the contribution of each resistance to the overall mass transfer resistance was also investigated. An increase in the liquid flow rate resulted in an increase of CO_2 flux for all membranes; the best contactor performance was obtained by using PSF-PVP membrane. It was concluded that addition of PVP to PSF membrane enhanced remarkably CO_2 flux up to 169% compred to the flux achieved by PSF membrane without PVP due to a drastic decrease in membrane resistance at the fixed liquid velocity. The results of the current study are promisining from several points of views. First, using membrane contactor, in general, provides an economical improvement compared to conventional amine based absorption processes with their major drawbacks. Seccond, among materials used for fabrication of membranes employed in CO_2 absorption, PSF offers economically a better option because it is cheaper than other materials such as PVDF. Finally, the novel membrane developed in this study can enhance the CO_2 caputure efficiency, and is an appropriate material with the potential to fulfill the demands of carbon dioxide absorption in gas-liquid membrane contactor applications. The absorption performance of the PSF-PVP membrane can be still improved by changing the polymer concentration in the dope solution, which its effects on the membrane surface structure and CO_2 absorption flux will be presented in our forthcoming paper. Further work is also ongoing on the use of amine-based absorbents for enhancing the CO_2 absorption performance in our laboratory. However, further work is required on the long-term stability of these membranes in detail to justify its use for large scale applications.

REFERENCES

1. A. Gabelman and S. T. Hwang, *J. Membr. Sci.*, **159**, 61 (1999).
2. T. E. Rufford, S. Smart, G. C. Y. Watson, B. F. Graham, J. Boxall, J. C. Diniz da Costa and E. F. May, *J. Petro. Sci. Eng.*, **94-95**, 123 (2012).
3. K. Lampert, A. Ziebik and W. Stanek, *Energy*, **35**, 1188 (2010).
4. S. H. Yeon, K. S. Lee, B. Sea, Y. I. Park and K. H. Lee, *J. Membr. Sci.*, **257**, 156 (2005).
5. J. A. Dunne, S. C. Jackson and J. Harte, in *Encyclopedia of Biodiversity 2nd Ed.* S. A. Levin Ed., Academic Press (2013).
6. W. Guo, F. Feng, G. Song, J. Xiao and L. Shen, *J. Nat. Gas. Chem.*, **21**, 633 (2012).
7. R. Naim and A. F. Ismai, *Sep. Purif. Technol.*, **115**, 152 (2013).
8. Y. Zhang, J. Sunarso, S. Liu and R. Wang, *Int. J. Greenh. Gas. Con.*, **12**, 84 (2013).
9. I. T. Pineda, J. W. Lee, I. Jung and Y. T. Kang, *Int. J. Refrig.*, **35**, 1402 (2012).
10. C. C. Lin and B. C. Chen, *Chem. Eng. Res. Des.*, **89**, 1722 (2011).
11. F. Yi, H. K. Zou, G. W. Chu, L. Shao and J. F. Chen, *Chem. Eng. J.*, **145**, 377 (2009).
12. H. H. Cheng and C. S. Tan, *Sep. Purif. Technol.*, **82**, 156 (2011).
13. E. Favre, *Chem. Eng. J.*, **171**, 782 (2011).
14. A. F. Ismail, T. D. Kusworo and A. Mustafa, *J. Membr. Sci.*, **319**, 306 (2008).
15. E. Favre, *J. Membr. Sci.*, **294**, 50 (2007).
16. A. Bottino, G. Capannelli, A. Comite, R. Di Felice and R. Firpo, *Sep. Purif. Technol.*, **59**, 85 (2008).
17. S. Khaisri, D. de Montigny, P. Tontiwachwuthikul and R. Jiraratananon, *J. Membr. Sci.*, **376**, 110 (2011).
18. C. A. Scholes, M. Simioni, A. Qader, G. W. Stevens and S. E. Kentish, *Chem. Eng. J.*, **195-196**, 188 (2012).
19. M. Modigell, M. Schumacher, V. V. Teplyakov and V. B. Zenkevich, *Desalination*, **224**, 186 (2008).
20. H. Y. Zhang, R. Wang, D. T. Liang and J. H. Tay, *J. Membr. Sci.*, **279**, 301 (2006).
21. P. T. Nguyen, E. Lasseuguette, Y. Medina-Gonzalez, J. C. Remigy, D. Roizard and E. Favre, *J. Membr. Sci.*, **377**, 261 (2011).
22. S. A. M. Marzouk, M. H. Al-Marzouqi, M. H. El-Naas, N. Abdullatif and Z. M. Ismail, *J. Membr. Sci.*, **351**, 21 (2010).
23. J. J. Cai, K. Hawboldt and M. A. Abdi, *J. Membr. Sci.*, **397-398**, 9 (2012).
24. Y. Zhang and R. Wang, *J. Membr. Sci.*, **452**, 379 (2014).
25. S. H. Lin, K. L. Tung, H. W. Chang and K. R. Lee, *Chemosphere*, **75**, 1410 (2009).
26. J. A. Franco, S. E. Kentish, J. M. Perera and G. W. Stevens, *Ind. Eng. Chem. Res.*, **50**, 4011 (2011).
27. S. Paul, A. K. Ghoshal and B. Mand, *Chem. Eng. J.*, **144**, 352 (2008).
28. S. Khaisri, D. deMontigny, P. Tontiwachwuthikul and R. Jiraratananon, *Sep. Purif. Technol.*, **65**, 290 (2009).
29. A. Mansourizadeh and A. F. Ismail, *Desalination*, **273**, 386 (2011).
30. S. Yan, M. X. Fang, W. F. Zhang, S. Y. Wang, Z. K. Xu, Z. Y. Luo and K. F. Cen, *Fuel Process. Technol.*, **88**, 501 (2007).
31. Y. Lv, X. Yu, J. Jia, S. T. Tu, J. Yan and E. Dahlquist, *Appl. Energy*, **90**, 167 (2012).
32. A. Mansourizadeh and A. F. Ismail, *J. Membr. Sci.*, **348**, 260 (2010).
33. Gh. Bakeri, T. Matsuura, A. F. Ismail and D. Rana, *Sep. Purif. Technol.*, **89**, 160 (2012).
34. N. Ghasem, M. Al-Marzouqi and L. Zhu, *Sep. Purif. Technol.*, **92**, 1 (2012).
35. M. Rahbari-Sisakht, A. F. Ismail and T. Matsuura, *Sep. Purif. Technol.*, **86**, 215 (2012).
36. E. Drioli, A. Criscuoli and E. Curcio, *Membrane Contactors: Fundamentals*, Applications and Potentialities, Elsevier (2006).
37. H. A. Rangwala, *J. Membr. Sci.*, **112**, 229 (1996).
38. E. R. Gilliland and T. K. Sherwood, *Ind. Eng. Chem.*, **26**, 516 (1934).
39. M. Mavroudi, S. P. Kaldis and G. P. Sakellaropoulos, *J. Membr. Sci.*, **272**, 103 (2006).
40. E. E. Wilson, *Trans. Am. Soc. Mech. Eng.*, **37**, 47 (1915).
41. S. Singh, K. C. Khulbe, T. Matsuura and P. Ramamurthy, *J. Membr. Sci.*, **142**, 111 (1998).

42. M. Amini, M. Jahanshahi and A. Rahimpour, *J. Membr. Sci.*, **435**, 233 (2013).
43. N. N. Li, A. G. Fane, W. S. W. Ho and T. Matsuura (Eds.), Wiley, New York (2008).
44. V. Y. Dindore, D. W. F. Brilman, P. H. M. Feron and G. F. Versteeg, *J. Membr. Sci.*, **235**, 99 (2004).
45. K. Kimmerle and H. Strathmann, *Desalination*, **79**, 283 (1990).
46. E. Fontananovaa, J. C. Jansen, A. Cristiano, E. Curcio and E. Drioli, *Desalination*, **192**, 190 (2006).
47. Y. Mansourpanah, K. Alizadeh, S. Madaeni, A. Rahimpour and H. SoltaniAfarani, *Desalination*, **271**, 169 (2011).
48. A. Mansourizadeh and A. F. Ismail, *J. Membr. Sci.*, **348**, 260 (2010).
49. M. Rahbari-sisakht, A. F. Ismail and T. Matsuura, *Sep. Purif. Technol.*, **88**, 99 (2012).
50. A. Xu, A. Yang, S. Young, D. deMontigny and P. Tontiwachwuthikul, *J. Membr. Sci.*, **311**, 153 (2008).
51. M. C. Yang and E. L. Cussler, *AIChE J.*, **32**, 1910 (1986).
52. A. Mansourizadeh and A. F. Ismail, *Int. J. Greenh. Gas. Con.*, **5**, 374 (2011).
53. S. H. Lin, C. F. Hsieh, M. H. Li and K. L. Tung, *Desalination*, **249**, 647 (2009).